

Mono- and Dinuclear Oxovanadium(V)calixarene Complexes and Their Activity as Oxidation Catalysts

Elke Hoppe, Christian Limberg,* and Burkhard Ziemer

Humboldt-Universität zu Berlin, Institut für Chemie, Brook-Taylor-Strasse 2, 12489 Berlin, Germany

Received June 20, 2006

The background of the investigation is constituted by reactive moieties and intermediates playing relevant roles on the surfaces of vanadiumoxide-based catalysts during the oxygenation/dehydrogenation of organic substrates. With the aim of modeling such species, a series of mono- and dinuclear charged and uncharged vanadium oxo complexes containing *p*-tert-butylated calix[4]arene and calix[8]arene ligands (denoted H_4B and H_8B'' , respectively, in the protonated forms) has been synthesized and characterized: $PPh_4[O=VB]$ (PPH_4^1), $O=VB^{OAc}$ (**2**), $PPh_4[O_2V_2HB'']$ (**3**), and $[\mu-O(O=V(OMe))_2B^{Me_2}]$ (**4**), where superscripts OAc and Me₂ indicate that one or two protons of H_4B are substituted by these residues, respectively. These compounds were analyzed both in solution and by means of single-crystal X-ray crystallography; it turned out that the crystal structures are retained on dissolution (**2** changed only from the paco to the cone structure). In the case of **4**, it could be shown that the bulk product consists of a mixture of two isomers (**4[†]** and **4[°]**) differing in the relative positions of the vanadium-bound methoxy groups. Subsequently, all compounds were tested as catalysts for the oxidation of alcohols with O₂. It turned out that the two dinuclear complexes efficiently catalyze the oxidation of 1-phenyl-1-propargyl alcohol and fluorenone; in addition, they even show some activity with respect to the oxidation of dihydroanthracene. This may hint to a higher activity of dinuclear sites on the surfaces of heterogeneous catalysts as well.

Introduction

Despite significant research efforts directed toward understanding the general features and reaction steps of oxidation catalysis mechanisms on surfaces, many systems can still be regarded as being poorly defined,¹ which may in part be due to the fact that a lot of difficulties are encountered during characterization of sites and reaction intermediates on surfaces.² Heterogeneous catalysts for oxidation reactions thus sometimes have to be employed as “black boxes”: Reactants are injected and products are formed in good yields with good selectivities, but a complete understanding of the origin of the catalytic behavior is not yet available.

For several years, we have been dealing with the modeling of surface intermediates occurring during heterogeneous oxidation processes with molecular compounds as well as

with the possibilities and limitations of such an approach.³ This contribution deals with reactive moieties playing relevant roles on the surfaces of vanadiumoxide-based catalysts during the oxidation of organic substrates. Various different surface species have been discussed as being active in one way or the other,⁴ and a representative example is the oxidative dehydrogenation (ODH) of methanol and

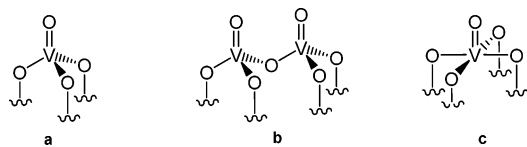
* To whom correspondence should be addressed. E-mail: christian.limberg@chemie.hu-berlin.de.

(1) Reitz, J. B.; Solomon, E. I. *J. Am. Chem. Soc.* **1998**, *120*, 11467.

(2) Hunger, M.; Weitkamp, J. *Angew. Chem.* **2001**, *113*, 3040; *Angew. Chem., Int. Ed.* **2001**, *40*, 2954.

(3) Limberg, C. *Angew. Chem.* **2003**, *115*, 6112; *Angew. Chem., Int. Ed.* **2003**, *42*, 5932. Hunger, M.; Limberg, C.; Kircher, P. *Angew. Chem.* **1999**, *111*, 1171; *Angew. Chem., Int. Ed.* **1999**, *38*, 1105. Hunger, M.; Limberg, C.; Kircher, P. *Organometallics* **2000**, *19*, 1044; Borgmann, C.; Limberg, C.; Cunsakis, S.; Kircher, P. *Eur. J. Inorg. Chem.* **2001**, 349; Hunger, M.; Limberg, C.; Kaifer, E.; Rutsch, P. *J. Organomet. Chem.* **2002**, *641*, 9. Limberg, C.; Hunger, M.; Habicht, W.; Kaifer, E. *Inorg. Chem.* **2002**, *41*, 3359. Roggan, S.; Limberg, C.; Ziemer, B. *Angew. Chem.* **2005**, *117*, 5393; *Angew. Chem., Int. Ed.* **2005**, *44*, 5259. Roggan, S.; Limberg, C.; Ziemer, B.; Brandt, M. *J. Organomet. Chem.* **2005**, *690*, 5282. Siewert, I.; Limberg, C.; Ziemer, B. *Z. Anorg. Allg. Chem.* **2006**, *632*, 1078. Wippert-Rodrigues, C.; Limberg, C.; Pritzkow, H. *Chem. Commun.* **2004**, 2734. Wippert-Rodrigues, C.; Limberg, C.; Pritzkow, H. *Eur. J. Inorg. Chem.* **2004**, 3644. Wippert Rodrigues, C.; Antelmann, B.; Limberg, C.; Pritzkow, H. *Organometallics* **2001**, *20*, 1825. Borgmann, C.; Limberg, C.; Kaifer, E.; Pritzkow, H.; Zsolnai, L. *J. Organomet. Chem.* **1999**, *580*, 214. Borgmann, C.; Limberg, C.; Zsolnai, L. *Chem. Commun.* **1998**, 2729.

Chart 1



alkanes for which vanadia on SiO_2 , Al_2O_3 , ZrO_2 , and other oxidic supports proved to be catalytically efficient.⁵ Some of the various working hypotheses are the following: the active and selective sites consist of mononuclear tetrahedrally coordinated V^{5+} (a in Chart 1) whereas dinuclear assemblies (like b in Chart 1) and polynuclear moieties are responsible for the loss in selectivity (oxygenation). On the other hand, species with a square pyramidal oxo coordination geometry around the vanadium center (c in Chart 1) have been proposed to initiate the oxidation of butane to MSA on vanadyl phosphate catalysts,⁶ and such units have been shown to form if vanadia is deposited on certain metal surfaces, too.⁷ We were interested in using these structural motifs as an inspiration for attempts to mimic them in molecular compounds. Two different ligand systems have established themselves in the past for the modeling of oxidic surfaces characteristic for transition-metal oxide catalysts or the support belonging to a certain catalyst: the deprotonated forms of silsesquioxanes⁸ ($\text{H}_3\text{A}^{\text{R}}$) and *p*-*tert*-butylated calixarenes⁹ (H_4B , $\text{H}_6\text{B}'$, $\text{H}_8\text{B}''$) (see Scheme 1).

After deprotonation, $\text{H}_3\text{A}^{\text{R}}$ represents a tripod ligand, whereas H_4B yields a tetrapodal ligand. Employing $\text{H}_3\text{A}^{\text{R}}$ and H_4B thus enables empathizing the embedding of a transition-metal ion in the midst of three or four oxo atoms of an oxidic surface (for instance, a support), respectively. On the other hand, ligands such as $[\text{B}']^{6-}$ or a calix[8]arene with eight phenolate units ($[\text{B}'']^{8-}$) provide more extended platforms of oxo atoms, where polynuclear moieties can arrange themselves, too.

With the aim of modeling a corresponding vanadium oxo single site, Feher and co-workers have already examined the vanadium chemistry of ligands $[\text{A}^{\text{R}}]^{3-}$. They were able to identify a corresponding $[\text{V}=\text{O}]^{3+}$ complex in solution, which, however, is involved in a dimerization equilibrium

Scheme 1

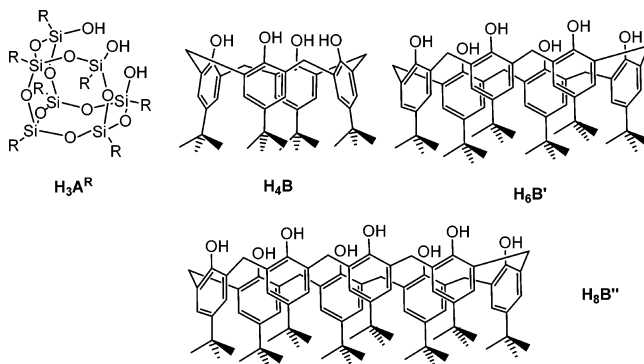
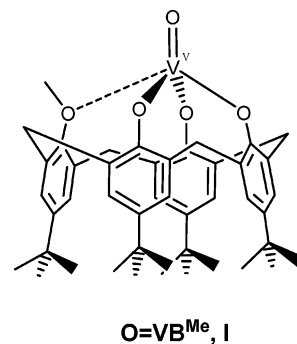


Chart 2



so that it could not be isolated as such.¹⁰ Vanadium oxo complexes of calix[4]arenes (B^{4-}) are not known. There is one example of a complex with a ligand derived from H_4B by monomethylation of a phenolic function, $\text{O}=\text{V}^{\text{VB}^{\text{Me}}}$ (**I**, see Chart 2)¹¹ and a few vanadium oxo compounds containing calix[3]-, calix[6]-, and calix[8]arene ligands are known, too, which, however, either are not homoleptic (i.e., the vanadium centers are wearing ligands with donor atoms other than O) or were not characterized structurally.¹²

Here, we describe our systematic studies concerning the preparation of calixarene oxovanadium complexes with varying nuclearity and the investigation of their reactivity and potential as structural or functional models for active sites on surfaces.

Experimental Section

General Procedures. All manipulations were carried out in a glovebox, or else by means of Schlenk-type techniques involving the use of a dry argon atmosphere. The ^1H , ^{13}C , and ^{51}V NMR spectra were recorded on a Bruker AV 400 NMR spectrometer (^1H , 400.13 MHz; ^{13}C , 100.63 MHz; ^{51}V , 105.25 MHz) with CH_2Cl_2 , CDCl_3 , or C_6D_6 as solvent at 20 °C. The ^1H NMR spectra were calibrated against the residual proton and natural abundance ^{13}C resonances of the deuterated solvent (CH_2Cl_2 δ_{H} 5.32 ppm, CDCl_3 δ_{H} 7.26 ppm, and C_6D_6 δ_{H} 7.15 ppm) and the ^{51}V NMR spectra

(4) Owens, L.; Kung, H. H. *J. Catal.* **1993**, *144*, 202. Evans, O. R.; Bell, A. T.; Tilley, T. D. *J. Catal.* **2004**, *226*, 292.

(5) (a) Comite, A.; Sorrentino, A.; Capannelli, G.; Di Serio, M.; Tesser, R.; Santacesaria, E. *J. Mol. Catal. A* **2003**, *198*, 151. (b) Zhou, R.; Cao, Y.; Yan, S.; Deng, J.; Liao, Y.; Hong, B. *Catal. Lett.* **2001**, *75*, 107. (c) Blasco, T.; Galli, A.; Lopez Nieto, J. M.; Trifido, F. *J. Catal.* **1997**, *169*, 203. (d) Arakawa, H.; Aresta, M.; Armor, J. N.; Barteau, M. A.; Beckman, E. J.; Bell, A. T.; Bercaw, J. E.; Creutz, C.; Dinjus, E.; Dixon, D. A.; Domen, K.; Dubois, D. L.; Eckert, J.; Fujita, E.; Gibson, D. H.; Goddard, W. A.; Goodman, D. W.; Keller, J.; Kubas, G. J.; Kung, H. H.; Lyons, J. E.; Manzer, L. E.; Marks, T. J.; Morokuma, K.; Nicholas, K. N.; Periana, R.; Que, L.; Rostrup-Nielson, J.; Sachtler, W. M. H.; Schmidt, L. D.; Sen, A.; Somorjai, G. A.; Stair, P. C.; Stults, B. R.; Tumas, W. *Chem. Rev.* **2001**, *101*, 953.

(6) Chen, B.; Munson, E. J. *J. Am. Chem. Soc.* **2001**, *124*, 1638.

(7) Schoiswohl, J.; Surnev, S.; Sock, M.; Ramsey, M. G.; Kresse, G.; Netzer, F. P. *Angew. Chem., Int. Ed.* **2004**, *43*, 5546.

(8) Lorenz, V.; Edelmann, F. T. *Z. Anorg. Allg. Chem.* **2004**, *630*, 1147; Copéret, C.; Chabanas, M.; Petroff Saint-Arroman, R.; Basset, J.-M. *Angew. Chem.* **2003**, *115*, 164. Feher, F. J.; Budzichowski, T. A. *Polyhedron* **1995**, *14*, 3239.

(9) RADIUS, U. *Z. Anorg. Allg. Chem.* **2004**, *630*, 957; Floriani, C. *Chem.—Eur. J.* **1995**, *5*, 19.

(10) Feher, F. J.; Walzer, J. F. *Inorg. Chem.* **1991**, *30*, 1689.

(11) (a) Hoppe, E.; Limberg, C.; Ziemer, B.; Mügge, C. *J. Mol. Catal. A* **2006**, *251*, 34; (b) Castellano, B.; Solari, E.; Floriani, C.; Scopelliti, R. *Inorg. Chem.* **1999**, *38*, 3406.

(12) (a) Gibson, V. C.; Redshaw, C.; Elsegood, M. R. *J. Chem. Soc., Dalton Trans.* **2001**, 767. (b) Hampton, P. D.; Daitch, C. E.; Alam, T. M.; Pruss, E. A. *Inorg. Chem.* **1997**, *36*, 2879. (c) Castellano, B.; Solari, E.; Floriani, C.; Scopelliti, R. *Inorg. Chem.* **1999**, *38*, 3406. Also see ref 20a.

against VOCl_3 as a standard. Microanalyses were performed on a Leco CHNS-932 elemental analyzer. Infrared (IR) spectra were recorded using samples prepared as KBr pellets with a Digilab Excalibur FTS 4000 FTIR-spectrometer.

Materials. Solvents were purified, dried, and degassed prior to use. Pure $n\text{Bu}_4\text{NVO}_3$,¹³ $\text{Ph}_4\text{P}[\text{VO}_2\text{Cl}_2]$,¹⁴ *p*-*tert*-butyl-calix[4]arene,¹⁵ dimethyl-*p*-*tert*-butyl-calix[4]arene,¹⁶ and *p*-*tert*-butyl-calix[8]arene¹⁷ were prepared according to the literature procedure.

$\text{VO}(\text{OCH}_3)_3$ was synthesized¹⁸ as described in the literature with some modifications: To a solution of 4.8 mL (0.05 mol) of VOCl_3 in 500 mL of toluene, heated to 80 °C, was added 6.1 mL (0.15 mol) of methanol while stirring. After 10 min, 21.1 mL (0.15 mol) of triethylamine was added. The suspension was stirred at 80 °C for another 15 min and then annealed to room temperature and stirred for an additional hour. All volatiles were evaporated under a vacuum and a temperature not higher than 40 °C. Sublimation of the green solid at 60 °C in static vacuo yielded 2.8 g (35%) of a yellow crystalline solid.

$n\text{Bu}_4\text{N}$ [*p*-*tert*-Butyl-calix[4]arene Tetrahydroxylato Oxovanadate(V)],^{Nbnd} **1.** Triethylamine (0.17 mL, 1.23 mmol) was added to a suspension of 200 mg (0.31 mmol) of *p*-*tert*-butyl-calix[4]arene, **H₄B**, in 5 mL of CH_2Cl_2 , and the resulting solution was treated dropwise with a solution of 210 mg (0.62 mmol) of $n\text{Bu}_4\text{NVO}_3$ in 5 mL of CH_2Cl_2 . After being stirred for 72 h at room temperature, the solution was evaporated to dryness and the resulting green-brown solid was extracted with diethyl ether (2 × 10 mL). Removal of all volatiles yielded a brown solid that was dissolved in 2–3 mL of acetone. This solution was cooled to –50 °C, which led to the precipitation of yellowish needles (that were discarded). The overlaying brown solution was separated via filtration, and evaporation of the solvent provided 172 mg (59% based on employed **H₄B**) of a crystalline brown solid (crude product). Further purification can be achieved via recrystallization (cooling of a saturated CH_2Cl_2 solution). This process, which leads to an analytically pure sample, is, however, time-consuming and accompanied by significant losses in yield.

¹H NMR (CDCl_3 , 297 K): δ 6.96 (s, 8H, H_{Ar}), 4.47 (d, ²*J* = 11.2 Hz, 4H, CH_2), 3.39 (m, 8H, $\text{N}-(\text{CH}_2)_4$), 2.99 (d, ²*J* = 11.2 Hz, 4H, CH_2), 1.65 (m, 8H, $\text{N}-(\text{CH}_2-\text{CH}_2)_4$), 1.42 (m, 8H, $\text{N}-(\text{CH}_2-\text{CH}_2-\text{CH}_2)_4$), 1.18 (s, 36H, $\text{C}(\text{CH}_3)_3$), 0.97 (t, ²*J* = 6 Hz, 12H, $\text{N}-(\text{CH}_2)_3-\text{CH}_3$). ¹³C NMR (CDCl_3 , 297 K): δ 156.2 (*q*- C_{Ar}), 140.1 (*q*- C_{Ar}), 127.5 (*q*- C_{Ar}), 121.4 (C_{Ar} -H), 56.3 ($\text{N}-(\text{CH}_2)_4$), 32.4 (CH_2), 31.4 ($\text{C}(\text{CH}_3)_3$), 29.2 ($\text{C}(\text{CH}_3)_3$), 21.7 ($\text{N}-(\text{CH}_2-\text{CH}_2)_4$), 17.27 ($\text{N}-(\text{CH}_2-\text{CH}_2-\text{CH}_2)_4$), 11.3 ($\text{N}-(\text{CH}_2)_3-\text{CH}_3$); ⁵¹V NMR (CDCl_3 , 297 K): δ –268. Anal. Found: C, 75.68; H, 9.94; N, 1.74. Calcd for $\text{C}_{60}\text{H}_{88}\text{NO}_5\text{V}$: C, 75.52; H, 9.29; N, 1.47. IR (KBr, cm^{-1}): 3047 (w), 2961 (s), 2872 (m), 1458 (s, br), 1420 (w), 1391 (w), 1391 (w), 1380 (m), 1360 (m), 1308 (m), 1283 (m), 1252 (m), 1204 (s), 1109 (w), 1030 (w), 978 (s), 920 (w), 883 (w), 870 (w), 829 (m), 798 (s), 758 (w), 727 (w), 696 (w), 677 (w), 544 (m), 498 (w), 432 (m), 422 (m).

Ph_4P [*p*-*tert*-Butyl-calix[4]arene Tetrahydroxylato Oxovanadate(V)],^{Pbnd} **1.** Synthesis of the deprotonated *p*-*tert*-butyl-calix[4]-

arene, **Li₄B**, was carried out according to the literature.¹⁹ *p*-*tert*-Butyl-calix[4]arene (3.66 g, 5.64 mmol), 0.16 g (22.5 mmol) of Li granulate and 2.89 g (22.5 mmol) of naphthalene were stirred in 60 mL of THF at room temperature overnight to give a pale orange solution. After all volatiles were removed, the remaining residue was washed with 30 mL of *n*-hexane and dried in vacuo, yielding 3.70 g (97%) of a white solid. This product was dissolved in 80 mL of toluene; the resulting solution was added to 2.67 g (5.47 mmol) of $\text{Ph}_4\text{P}[\text{VO}_2\text{Cl}_2]$ via cannula. After being refluxed for 20 h, the brown suspension was allowed to cool to room temperature. After all volatiles were removed, the remaining solid was washed with 80 mL of CH_3OH and dried again. It was then redissolved in 30 mL of CH_2Cl_2 and precipitated by the addition of *n*-hexane, yielding 4.98 g (85%) of a green, glittering solid.

¹H NMR (CD_2Cl_2 , 297 K): δ 7.89 (m, 4H, Ph_4P^+), 7.76 (m, 8H, Ph_4P^+), 7.66 (m, 8H, Ph_4P^+), 6.95 (s, 8H, H_{Ar}), 4.38 (d, ²*J* = 11.2 Hz, 4H, CH_2), 2.91 (d, ²*J* = 11.2 Hz, 4H, CH_2), 1.18 (s, 36H, $\text{C}(\text{CH}_3)_3$). ¹³C NMR (CD_2Cl_2 , 197 K): δ 158.9 (*q*- C_{Ar}), 143.0 (*q*- C_{Ar}), 136.1 (d, *J* = 3 Hz, Ph_4P^+), 134.9 (d, *J* = 10 Hz, Ph_4P^+), 131.0 (d, *J* = 13 Hz, Ph_4P^+), 130.5 (*q*- C_{Ar}), 123.8 (C_{Ar} -H), 118.0 (d, *J* = 89 Hz, Ph_4P^+), 34.7 (CH_2), 34.1 ($\text{C}(\text{CH}_3)_3$), 31.8 ($\text{C}(\text{CH}_3)_3$). ³¹P NMR (CD_2Cl_2 , 297 K): δ 23.76. ⁵¹V (CD_2Cl_2 , 297 K): δ –297. Anal. Found: C, 72.52; H, 6.79; Cl, 6.55. Calcd for $\text{C}_{68}\text{H}_{72}\text{O}_5\text{PV}$ CH_2Cl_2 : C, 72.94; H, 6.56; Cl, 6.24. Mp: 368 °C. IR (KBr, cm^{-1}): 3046 (w), 2952 (s), 2918 (m), 2865 (m), 1587 (w), 1457 (s), 1441 (m), 1392 (w), 1361 (m), 1310 (m), 1286 (m), 1260 (s), 1207 (s), 1110 (s), 993 (s), 869 (w), 830 (m), 799 (s), 755 (w), 724 (s), 688 (m), 546 (m), 526 (s), 501 (w), 426 (s).

Oxo[O-acetyl-*p*-*tert*-butyl-calix[4]arene-trihydroxylato]vanadium(V), **2.** A solution of CH_3COCl (0.5 mL, 0.96 M) in CH_2Cl_2 (0.48 mmol) was added to a solution of 250 mg (0.24 mmol) of **PPh₄1** in 10 mL of CH_2Cl_2 . Within 10 min, the color of the solution changed from yellow-green to red-brown. After being stirred for another 15 min, all volatiles were evaporated; the residual solid was extracted with *n*-hexane (5 mL). This led to a ruby-colored solution that was filtered from a pale mauve solid (predominantly $\text{Ph}_4\text{P}^+\text{Cl}^-$). Removing the solvent from the filtrate yielded 160 mg (89%) of a red solid.

¹H NMR (CDCl_3 , 297 K): δ 7.25 (d, ⁴*J* = 2.4 Hz, 2H, H_{Ar}), 7.16 (d, ⁴*J* = 2.4 Hz, 2H, H_{Ar}), 6.94 (s, 2H, H_{Ar}), 6.90 (s, 2H, H_{Ar}), 4.59 (d, ²*J* = 13.5 Hz, 2H, CH_2), 4.37 (d, ²*J* = 13.1 Hz, 2H, CH_2), 3.37 (d, ²*J* = 13.1 Hz, 2H, CH_2), 3.19 (d, ²*J* = 13.5 Hz, 2H, CH_2), 2.63 (s, 3H, $\text{CH}_3\text{C}(\text{O})$), 1.42 (s, 18H, $\text{C}(\text{CH}_3)_3$), 0.90 (s, 9H, $\text{C}(\text{CH}_3)_3$), 0.82 (s, 9H, $\text{C}(\text{CH}_3)_3$). ¹³C NMR (CDCl_3 , 297 K): δ 167.9 (C_{Ar}), 161.3 (C_{Ar}), 154.0 (C_{Ar}), 147.8 (C_{Ar}), 147.1 (C_{Ar}), 144.9 (C_{Ar}), 142.0 (C_{Ar}), 130.7 (C_{Ar}), 129.8 (C_{Ar}), 125.9 (C_{Ar}), 125.1 (C_{Ar}), 124.7 (C_{Ar} -H), 124.4 (C_{Ar} -H), 124.3 (C_{Ar} -H), 124.2 (C_{Ar} -H), 33.0 ($\text{C}(\text{O})\text{CH}_3$), 32.6 ($\text{C}(\text{CH}_3)_3$), 32.5 ($\text{C}(\text{CH}_3)_3$), 31.7 (CH_2), 31.6 (CH_2), 30.4 ($\text{C}(\text{CH}_3)_3$), 29.5 ($\text{C}(\text{CH}_3)_3$), 29.3 ($\text{C}(\text{CH}_3)_3$). ⁵¹V NMR (C_6D_6 , 297 K): δ –460 (s, br). Anal. Found: C, 74.01; H, 9.49. Calcd for $\text{C}_{46}\text{H}_{55}\text{O}_6\text{V}$ 1.5 C_6H_{14} : C, 74.71; H, 8.66. Mp: 128 °C (dec). IR (KBr, cm^{-1}): 3524 (m), 3048 (w), 2960 (s), 2905 (m), 2868 (w), 1751 (s), 1481 (s), 1461 (m), 1393 (w), 1364 (s), 1280 (m, br), 1206 (s, br), 1119 (m), 1012 (m), 996 (m), 943 (w), 922 (w), 871 (m), 818 (w), 799 (w), 694(vw), 596 (vw).

Ph_4P [*p*-*tert*-butyl-calix[8]arene heptahydroxylato dioxovanadate(V)], **3.** *p*-*tert*-Butyl-calix[8]arene (2.00 g, 1.5 mmol) and 0.43 mL (3.1 mmol) of triethylamine were added to a solution of 1.52 g (3.1 mmol) of $\text{Ph}_4\text{P}[\text{VO}_2\text{Cl}_2]$ in 80 mL of acetonitrile. After being stirred at room temperature for 5 h, the black solution was

(13) Day, V. W.; Klempner, W. G.; Yagasaki, A. *Chem. Lett.* **1990**, *19*, 1267.

(14) (a) Ehrlich, P.; Engel, W. *Z. Anorg. Allg. Chem.* **1963**, *322*, 217. (b) Fenske, D.; Shihada, A.-F.; Schwab, Dehnicke, K. *Z. Anorg. Allg. Chem.* **1980**, *471*, 140.

(15) Gutsche, C. D.; Iqbal, M. *Org. Synth.* **1993**, *CV 8*, 75.

(16) Gutsche, C. D.; Dhawan, B.; Levine, J. A.; No, K. H.; Bauer, L. J. *Tetrahedron* **1983**, *39*, 409.

(17) Munch, J. H.; Gutsche, C. D. *Org. Synth.* **1993**, *CV 8*, 80.

(18) Funk, H.; Weiss, W.; Zeising, N. *Z. Anorg. Allg. Chem.* **1958**, *295*, 327.

(19) Guillemot, G.; Solari, E.; Rizzoli, C.; Floriani, C. *Chem.—Eur. J.* **2002**, *8*, 2072.

Table 1. Crystal Data and Experimental Parameters for the Crystal Structure Analyses of Ph4P1, 2, 3, and 4

	Ph4P1	2	3	4
formula	C ₆₈ H ₇₂ O ₅ PV CH ₂ Cl ₂	C ₄₆ H ₅₅ O ₆ V	C ₁₂₆ H ₁₄₆ N ₇ O ₁₀ PV ₂	C ₄₈ H ₆₄ O ₉ V ₂
fw (g mol ⁻¹)	1136.09	754.84	2051.35	886.99
T (K)	150(2)	180(2)	150(2)	180(2)
wavelength (Å)	0.71073	0.71073	0.71073	0.71073
cryst syst	tetragonal	monoclinic	monoclinic	orthorhombic
space group	<i>P4/n</i>	<i>P2₁/a</i>	<i>P2₁/n</i>	<i>Pbcn</i>
<i>a</i> (Å)	12.763(3)	11.752(2)	17.0125(3)	20.447(2)
<i>b</i> (Å)	12.763(3)	29.076(4)	28.8155(7)	11.381(2)
<i>c</i> (Å)	18.733(9)	12.547(2)	23.6724(4)	20.263(2)
α (deg)	90	90	90	90
β (deg)	90	104.94(2)	99.1190(10)	90
γ (deg)	90	90	90	90
<i>V</i> (Å ³)	3050(2)	4142.2(10)	11458.1(4)	4715.3(8)
<i>Z</i>	2	4	4	4
<i>D</i> (g cm ⁻³)	1.237	1.210	1.189	1.089
μ (MoKα) (mm ⁻¹)	0.326	0.286	0.238	0.252
<i>F</i> (000)	1200	1608	4368	1656
GOF	1.047	0.879	1.123	0.914
R _{ind} [<i>I</i> > 2σ(<i>I</i>)]	R1 = 0.0402, wR2 = 0.1020	R1 = 0.0454 wR2 = 0.0925	R1 = 0.0689 wR2 = 0.1594	R1 = 0.0596 wR2 = 0.1568
R _{ind} (all data)	R1 = 0.0550 wR2 = 0.1135	R1 = 0.0863 wR2 = 0.1033	R1 = 0.0862 wR2 = 0.1677	R1 = 0.1051 wR2 = 0.1741
Δρ _{min} /Δρ _{max} (e Å ⁻³)	-0.429/0.624	-0.392/0.632	-0.648/1.905	-0.350/0.667

filtered and all volatiles were evaporated. The resulting black solid was crystallized by cooling an acetonitrile solution, yielding 2.25 g (83%) of pure **3**.

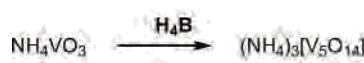
The ¹H and ¹³C NMR spectroscopic data are in agreement with those described in the literature²⁰ before. Anal. Found: C, 74.07; H, 7.04; N, 3.37. Calcd for C₁₁₂H₁₂₅O₁₀PV₂·5CH₃CN: C, 74.41; H, 7.16; N, 3.55. Mp: >300 °C.

Dimethoxy-dioxo-μ-oxo[1,3-dimethyl-*p*-tert-butyl-calix[4]arene-dihydroxylato]divanadium(V), 4. An orange solution of 0.50 g (3.1 mmol) of OV(OCH₃)₃ and 1.06 g (1.6 mmol) of 1,3-dimethyl-*p*-tert-butyl-calix[4]arene in 40 mL of THF was heated under reflux for one night. The solution's color changed to darkish red. All volatiles were evaporated to dryness; the resulting solid was extracted with acetonitrile and all volatiles were again evaporated. The residual red solid was redissolved in 10 mL of CH₂Cl₂, and after the addition of 30 mL of *n*-hexane, the solution was concentrated in a vacuum until small amounts of a red precipitate appeared. Cooling of the solution overnight to 5 °C yielded 1.1 g (80%) of a crude product **4**. A pure sample could be obtained by recrystallization from a CH₂Cl₂/*n*-hexane solution and washing with small amounts of *n*-hexane.

¹H NMR (CDCl₃, 297 K, **4**): δ 5.11 (s, 6H, VOCH₃), 4.36 (d, 2H, ²*J* = 12.5 Hz, CH₂), 4.09 (s, 3H, C_{Ar}OCH₃), 4.05 (d, 2H, ²*J* = 12.5 Hz, CH₂), 3.84 (s, 3H, C_{Ar}OCH₃), 3.36 (d, 2H, ²*J* = 12.5 Hz, CH₂), 3.14 (d, 2H, ²*J* = 12.5 Hz, CH₂), 1.35 (s, 18H, CCH₃), 0.84 (s, 9H, CCH₃), 0.81 (s, 9H, CCH₃). ¹H NMR (CDCl₃, 297 K, **4**): δ 5.16 (s, 6H, VOCH₃), 5.10 (d, 2H, ²*J* = 12.5 Hz, CH₂), 4.32 (d, 2H, ²*J* = 12.5 Hz, CH₂), 3.94 (s, 6H, C_{Ar}OCH₃), 3.36 (d, 2H, ²*J* = 12.5 Hz, CH₂), 3.15 (d, 2H, ²*J* = 12.5 Hz, CH₂), 1.35 (s, 18H, CCH₃), 0.82 (s, 18H, CCH₃).

Because of serious overlap, the signals for the aryl protons cannot be assigned unambiguously to the cis and trans isomers in CDCl₃ as the solvent (which, however, better resolves the other regions). They appear in the form of multiplets of equal integral at δ 7.23 (m, H_{Ar}), 7.10 (m, H_{Ar}), 6.64 (m, H_{Ar}), 6.56 (m, H_{Ar}). In C₆D₆ solution, the corresponding signals can be assigned:

Scheme 2



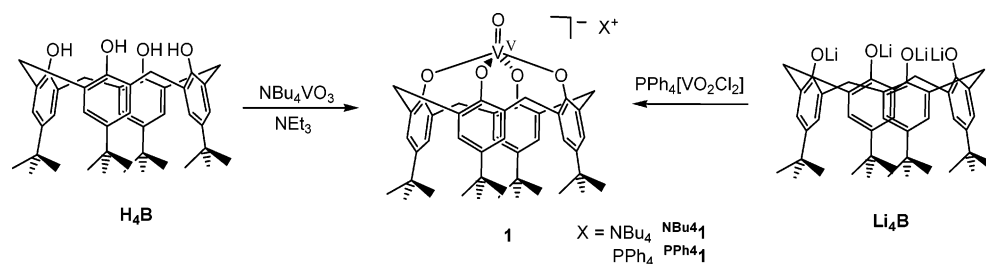
¹H NMR (C₆D₆, 297 K, **4**): δ 7.30 (d, 2H, ⁴*J* = 2.0 Hz, H_{Ar}), 7.22 (d, 2H, ⁴*J* = 2.3 Hz, H_{Ar}), 6.87 (d, 2H, ⁴*J* = 2.0 Hz, H_{Ar}), 6.81 (d, 2H, ⁴*J* = 2.3 Hz, H_{Ar}).

¹H NMR (C₆D₆, 297 K, **4**): δ 7.28 (d, 2H, ⁴*J* = 2.3 Hz, H_{Ar}), 7.24 (d, 2H, ⁴*J* = 2.3 Hz, H_{Ar}), 6.84 (s(br), 4H, H_{Ar}). ¹³C NMR (CDCl₃, 297 K): δ 168.5, 168.3, 152.7, 146.3, 145.8, 133.2, 133.0, 132.6, 132.4, 128.1 (C_{Ar}-H), 126.4(C_{Ar}-H), 126.2(C_{Ar}-H), 126.1-(C_{Ar}-H), 125.9(C_{Ar}-H), 125.5 (C_{Ar}-H), 123.7 (C_{Ar}-H), 75.2 (VOCH₃), 63.4 (OCH₃), 63.0 (OCH₃), 53.0 (C(CH₃)₃), 34.5 (CH₂), 33.9 (CH₂), 31.9(C(CH₃)₃), 31.2 (C(CH₃)₃). ⁵¹V NMR (C₆D₆, 297 K): δ -542. Anal. Found: C, 65.73; H, 7.32. Calcd for C₄₈H₆₄O₉V₂: C, 65.00; H, 7.27. IR (KBr, cm⁻¹): 3047 (w), 2961 (s), 2920 (m), 2866 (w), 2820 (w), 1481 (s, br), 1362 (m), 1313 (w), 1300 (w), 1250 (m), 1207 (s), 1123 (m), 1059 (s), 1017 (m), 995 (m), 941 (w), 918 (w), 860 (m), 813 (vs), 798 (vs), 775 (w), 696 (w), 648 (w), 635 (m), 625 (w), 588 (w).

Protocol for the Oxidation Studies. Catalyst (0.01 mmol) was dissolved in 1.5 mL of acetonitrile. After the addition of 500 mg of molecular sieve powder (3 Å), 1.00 mmol alcohol in 0.5 mL of acetonitrile was added. Subsequently, the mixture was stirred vigorously for 3 h (or for 1 h when 3 h led to a complete conversion) at 80 °C under a dioxygen atmosphere (oxygen was allowed to pass through the reaction vessel for 15 s before the reaction, and this procedure was repeated every 60 min). The mixture was then cooled to room temperature, and the molecular sieve powder was separated via filtration. In the case of high boiling alcohols (and resulting carbonyl compounds), the acetonitrile solvent was then simply evaporated in a vacuum. The conversion was determined by ¹H NMR spectroscopy. In the case of low boiling alcohols, the

(20) (a) Hofmeister, G. E.; Hahn, F. E.; Pedersen, S. F. *J. Am. Chem. Soc.* **1989**, *111*, 2318. (b) Hofmeister, G. E.; Alvarado, E.; Leary, J. A.; Yoon, D. I.; Pedersen, S. F. *J. Am. Chem. Soc.* **1990**, *112*, 8843.

Scheme 3



reaction mixture was filtered and directly employed in ^1H NMR spectroscopic investigations.

All starting materials and products are known and commercially available. The turnover frequencies (abbreviated TOF) were calculated as the number of moles of substrate that a mole of catalyst can convert per unit time.

Crystal Structure Determinations Suitable crystals of $\text{NBu}_4\text{1}$ could be obtained by cooling a saturated solution in CH_2Cl_2 to -30°C . Single crystals of $\text{PPh}_4\text{1}$ and **5** were obtained by diffusion of *n*-hexane at room temperature into a CH_2Cl_2 solution of $\text{PPh}_4\text{1}$ and **5**, respectively. Suitable crystals of **2** were obtained by evaporation of the solvent from a saturated hexane solution. Single crystals of **3** were obtained by cooling a saturated acetonitrile solution at 5°C . Crystals of **4** were obtained by evaporation of the solvent from a saturated acetonitrile solution at room temperature. The crystals were mounted on a glass fiber and then transferred into the cold nitrogen gas stream of the diffractometer (Stoe Stadi for $\text{PPh}_4\text{1}$, Stoe IPDS for $\text{NBu}_4\text{1}$, **2**, and **4**, Stoe IPDS2T for **3** and **5**) using $\text{MoK}\alpha$ radiation, $\lambda = 0.71073 \text{ \AA}$, and the structures were solved by direct methods (SHELXS-97),²¹ refined versus F^2 (SHELXL-97)²² with anisotropic temperature factors for all non-hydrogen atoms (Table 1). All hydrogen atoms were added geometrically and refined by using a riding model (except for H113 in the crystal structure of **3**, which was found).

The crystallographic data (apart from structure factors) of $\text{NBu}_4\text{1}$, $\text{PPh}_4\text{2}$, **3**, and **4** were deposited at the Cambridge Crystallographic Data Center as supplementary publications CCDC 610225, 610226, 610227, 610228, and 610229, respectively. Copies of the data can be ordered free of charge on application to CCDC, 12 Union Road, Cambridge CB2 1EZ (fax: 44-1223-336-033; E-mail: deposit@ccdc.cam.ac.uk).

Results and Discussion

Syntheses and Structures of Mono- and Dinuclear Calixarene Vanadium Oxo Complexes. For the above-mentioned purpose first of all a set of various different calixarene vanadium oxo complexes had to be prepared. To obtain a complex containing an $\text{O}=\text{V}^{3+}$ unit embedded in a tetragonal oxo coordination environment, we reacted tetrabutylammonium metavanadate with H_4B . This, however, led in good yields to the isolation of a pentanuclear vanadate **II** (as evidenced by single-crystal X-ray analysis) that first caught attention²³ in 1989, as it represented a novel type of structure in polyoxometallate chemistry being based on corner-sharing tetrahedrons (see Scheme 2). Obviously, the

contact of the metavanadate starting material with the acidic protons in H_4B triggers aggregation and condensation reactions leading to **II** instead of a calixarene complex. Hence, in the next attempt, NEt_3 was added as a base, which indeed enabled formation of the envisioned complex $\text{NBu}_4\text{[O=VB]}$, $\text{NBu}_4\text{1}$, (Scheme 3) in good yields. However, it is difficult to completely separate $\text{NBu}_4\text{1}$ from small amounts of unreacted H_4B during the workup procedure. Analytically pure $\text{NBu}_4\text{1}$ can be obtained via crystallization by cooling a CH_2Cl_2 solution but only if significant losses in yield are accepted. Alternatively, the complex anion **1** can be synthesized starting from the lithium salt Li_4B , which can be obtained via reaction of H_4B with lithium naphthalenide: Corresponding treatment with tetraphenylphosphonium dichlorodioxovanadate $\text{PPh}_4[\text{VO}_2\text{Cl}_2]$ leads to the elimination of LiCl (and apparently also Li_2O), yielding $\text{PPh}_4[\text{O=VB}]$, $\text{PPh}_4\text{1}$, (Scheme 3) for which an X-ray crystal structure analysis was performed (see Figure 1). As expected, the vanadyl group in **1** is surrounded symmetrically by an O_4 donor set, and **1** therefore represents the first model for such a situation on an oxidic support.

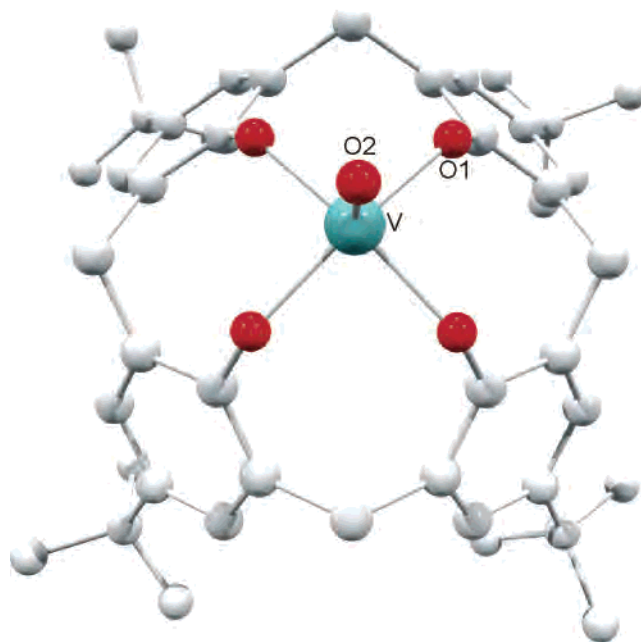


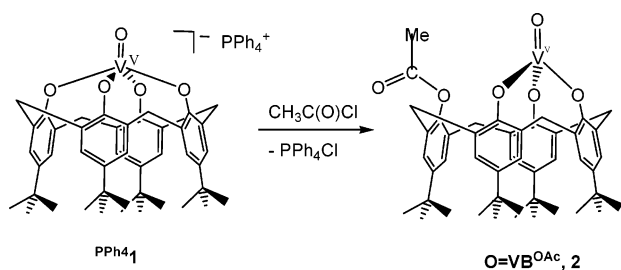
Figure 1. Molecular structure of the anion of $\text{PPh}_4\text{1}$. All hydrogen atoms, the Ph_4P^+ cation, and a cocrystallized solvent molecule CH_2Cl_2 were omitted for clarity. The molecule contains a crystallographic C_4 axis through V and O2. Selected bond distances (\AA) and angles (deg): V–O2, 1.5917(8); V–O1, 1.8858(4); V–O4, 0.3690(5); $\text{C}_{\text{Ar}}\text{–O1–V}$, 133.144(10); $\text{O2}=\text{V–O1}$, 101.285(13).

(21) Sheldrick, G. M. *SHELXS-97 Program for Crystal Structure Solution*; University of Göttingen: Göttingen, Germany, 1997.

(22) Sheldrick, G. M. *SHELXL-97 Program for Crystal Structure Refinement*; University of Göttingen: Göttingen, Germany, 1997.

(23) Day, V. W.; Klemperer, W. G.; Yaghi, O. M. *J. Am. Chem. Soc.* **1989**, *111*, 4518.

Scheme 4



The cavity hosts a CH_2Cl_2 molecule, and the coordination sphere around the vanadium atom can be described as being almost ideal square pyramidal: as a crystallographic C_4 axis runs through V and O2, all V–O_{Ar} bonds have the same length (1.8858(4) Å). However, the V center is not located in the plane formed by the corresponding four O atoms but 0.3690(5) Å above it. The terminal V–O2 bond distance (1.5917(8) Å) is very similar to that in **1** (1.598(5) Å), whereas the other V–O bonds are somewhat longer than comparable bonds in **1** (1.793(5), 1.811(6), and 1.825(5) Å).

PPh₄1 and **NBu₄1** are comparatively stable compounds that can even be handled in air for short periods of time. **PPh₄1** does not react with alcohols such as ethanol and methanol, and the solid is stable against water. According to the NMR data, **1** shows in solution the same structure as in the crystalline state: Singlet signals for the *t*Bu protons and the aryl protons as well as the fact that only two doublets are observed for the methylene protons point to a C_4 symmetry, as expected from the results of X-ray crystallography.

The ^{51}V NMR signal appears at –268 ppm for **NBu₄1** in CDCl_3 and at –297 ppm for **PPh₄1** in CD_2Cl_2 , i.e., shifted to lower field in comparison to the known neutral compound **1** (–352 ppm).^{11a}

For comparative reactivity studies, it seemed desirable to also investigate a neutral calix[4]arene vanadium(V) oxo complex. As mentioned, so far one representative has been described (**1**) that, however, is difficult to isolate in the pure state free from V^{IV} impurities.¹¹ Hence, we contemplated the synthesis of a more easily accessible derivative. Indeed, starting from **PPh₄1**, such a neutral complex can be obtained in a clean and facile synthesis: the addition of $\text{CH}_3\text{C}(\text{O})\text{Cl}$ leads to the precipitation of PPh_4Cl and formation of $\text{O}=\text{VB}^{\text{OAc}}$, **2** (see Scheme 4). The result of an X-ray crystal analysis is shown in Figure 2.

Whereas the coordination geometry around V in **1** has to be described most appropriately as being distorted trigonal bipyramidal because of the fact that the methoxy group binds at a longer distance to V too (compare Chart 2), the vanadium center in **2** is coordinated tetrahedrally by the O atoms O2, O3, O4, and O5; there is no interaction with the O atom of the acetyl unit ($d = 3.040(2)$ Å), and consequently, **2** can be regarded as modeling species a in Chart 1. However, both complexes **1** and **2** show almost equal V=O bond lengths; the bonds to the aryloxy O atoms are somewhat shorter in **2** (1.753(2), 1.798(2), and 1.785(2) Å) than in **1** (1.793(5), 1.811(6), and 1.825(5) Å). As found in one of the molecular structures reported for **1**,^{11a} the calixarene moiety in crystal-

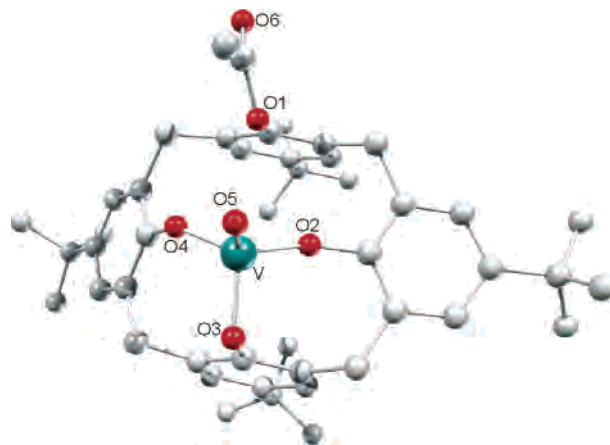


Figure 2. Molecular structure of complex **2**. All hydrogen atoms were omitted for clarity. Selected bond distances (Å) and angles (deg): O1–V, 3.040(2); O2–V, 1.753(2); O3–V, 1.798(2); O4–V, 1.785(2); O5–V, 1.596(2); O1–V–O5, 79.89(8); O2–V–O3, 102.61(8); O2–V–O4, 115.95(9); O2–V–O5, 113.60(10); O3–V–O4, 110.34(9); O3–V–O5, 104.36(10); O4–V–O5, 109.14(10); C_{Ar}–O1–V, 99.04(13); C_{Ar}–O2–V, 206.0(2); C_{Ar}–O3–V, 106.5(2); C_{Ar}–O4–V, 145.5(2); Ar(O1)–Ar(O3), 15.42(11); Ar(O2)–Ar(O4), 59.45(11).

line **2** adopts the partial cone (so-called “paco”) conformation ($C_{\text{Ar}}\text{–V–O2} = 206.0(2)^\circ$). Often, the corresponding “cone” structures (with C_s symmetry) are very close in energy, so that sometimes even both conformations are observed in the solid depending on the conditions of crystallization,^{11a} and, furthermore, a situation favored in the solid (where packing effects occur) might not be the one favored in solution. Interconversion is possible in solution so that the most stable structure is adopted if the activation barrier is not too high. This is indeed the case for **2**.

In the ^1H NMR spectrum, three signals in the ratio 2:1:1 can be observed for the protons of the *t*Bu groups, and for the methylene protons, two pairs of doublets are found, indicating a C_s symmetry with a mirror plane running through the C_{Ar}–OAc moiety, the V=O group, and the phenolic unit opposite to the acetylated V–O–C_{Ar} group. This suggests that the cone structure is preferred in solution (or that all phenoxy ligands in **2** switch very rapidly so that an averaged spectrum is observed on the NMR time scale). In a C_s symmetric structure, the two protons of the two different aryl rings halved by the mirror plane should be magnetically equivalent and show one singlet per aryl ring. The remaining two aryl rings should be equivalent, but not the two protons within an individual unit. Hence, for these two rings, two doublets should be observed. This is exactly what is found experimentally in the region where the aryl protons absorb, which again points to a cone conformation.

The chemical shift in the ^{51}V NMR spectrum amounts to –460 ppm, i.e., the signal is shifted by more than 100 ppm to higher field in comparison to **1**. Comparing the series **2**, **1**, and **1**, it thus has to be noted that starting from a tetrahedrally coordinated vanadyl group (**2**), via weak coordination of an additional ligand (**1**), up to strong coordination (**1**) leads to an increased deshielding of the vanadium center. It is difficult to elucidate the exact reasons for this trend, because structure and electronics change simultaneously.

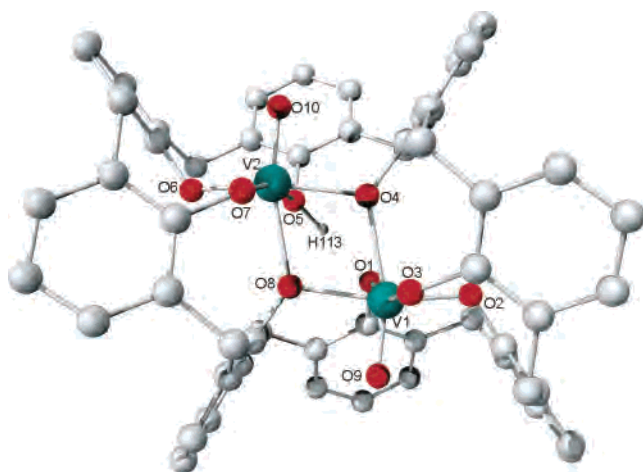
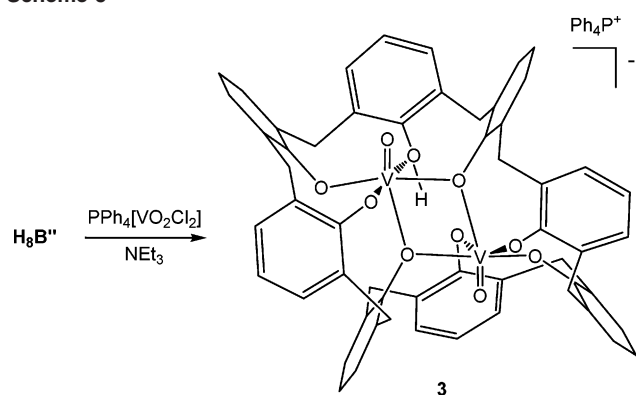


Figure 3. Molecular structure of the anion of **3**. All hydrogen atoms, the *tert*-butyl groups, and cocrystallized solvent molecules (acetonitrile) were omitted for clarity. Selected bond distances (Å) and angles (deg): O1–V1, 2.036(2); O2–V1, 1.849(2); O3–V1, 1.852(2); O4–V1, 2.212(2); O8–V1, 1.992(2); O9–V1, 1.589(2); O5–V2, 2.141(2); O6–V2, 1.836(2); O7–V2, 1.841(2); O4–V2, 1.968(2); O8–V2, 2.174(2); O10–V2, 1.599(2); O5–H113, 0.93(8); O1–H113, 1.61(8); O5–H113–O1, 177(7); V1–O4–V2, 107.20(8); V1–O8–V2, 107.77(8); V1–O₄(O1, O2, O3, O8), 0.2313(4); V2–O₄(O4, O5, O6, O7), 0.2202(4).

Scheme 5



Like **1**, compound **2** shows only a slight sensitivity toward oxygen, but it is very sensitive to water. In the absence of both, it is stable in solution for long periods.

We next turned our attention to the synthesis of compounds containing two oxovanadium units to also allow for a comparison of the reactivity of dinuclear vs mononuclear complexes. Accordingly, higher calixarenes were employed as starting materials, as these offer room for more than one vanadium center. First of all, **H₈B''** was chosen to be reacted with $\text{PPh}_4[\text{VO}_2\text{Cl}_2]$ in the presence of Et_3N as a base. The resulting product was fully characterized, and a single-crystal X-ray analysis revealed the structure (Figure 3 and Scheme 5) and constitution of $\text{PPh}_4[\text{O}_2\text{V}_2\text{HB}'']$, **3**.

It turned out that a salt containing the anion of **3** in combination with a different cation had been reported before by Pedersen and co-workers²⁰ as the product of the conversion of $\text{VO}(\text{O}^i\text{Pr})_3$ with **H₈B''** in the presence of (*R*)-(+)-1-(1-naphthyl)ethylamine. A single-crystal X-ray diffraction study had not been performed, but the solution structure of **3** had been investigated in detail. A suggestion for a structure was finally made on the basis of a structure determination

for a similar titanium complex; this proposed structure is identical with the one determined here by X-ray crystallography.

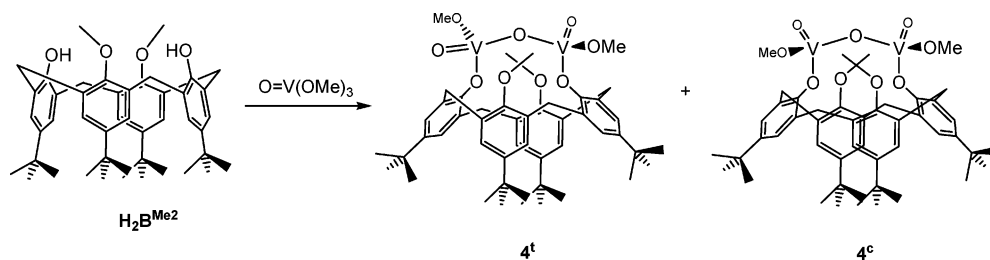
The formation of **3** must have proceeded via the addition of OH functions to $\text{V}=\text{O}$ groups under elimination of HCl and water (a similar type of reactivity has been reported only recently for molybdenyl chemistry)²⁴ so that two at first independent $\text{O}=\text{V}^{3+}$ units are coordinated by four aryloxy ligands each, as in **1**. However, two facts prohibit a description of **3** as a dinuclear version of **1**: First, one of the phenol functions in **H₈B''** is not deprotonated (i.e., a coordinated alcohol function results), so that **3** contains only a monoanion, and second, the ligand folds in a way that allows for the coordination of five phenoxy functions at the vanadium centers; that is, two of them within **3** adopt a bridging binding modus. At the remaining coordination sites, the terminal oxo ligands (O9 and O10) are bonded, being positioned in a cavity defined by three aryl rings; the two vanadium atoms are thus located in pseudooctahedral environments. As mentioned already, at one of the calixarene oxygen atoms (O5), a proton (H113) remained bonded, which could be located in the crystal structure analysis ($\text{O}-\text{H} = 0.93(8)$ Å); it undergoes a hydrogen bond to the opposite calixarene oxygen atom ($\text{H}\cdots\text{O1} = 1.61(8)$ Å, $\text{O5}-\text{H113}\cdots\text{O1} = 177(7)^\circ$). The vanadium atoms V1 and V2 are positioned somewhat (0.2312(4) and 0.2202(4) Å) above the ideal planes through O1, O2, O3, O8 and O4, O5, O6, O7, respectively. The terminal $\text{V}=\text{O}$ bond distances ($\text{V1}-\text{O9} = 1.589(2)$ Å, $\text{V2}-\text{O10} = 1.599(2)$ Å) lie in the usual range, being comparable to those displayed by **1**, **1**, and **2**. The distance between the two vanadium atoms amounts to 3.3677(7) Å.

Having accessed a dinuclear, singly charged vanadium oxo complex, we also pursued the syntheses of a corresponding neutral complex, ideally containing $\text{V}-\text{O}-\text{V}$ units. Refluxing **H₂B^{Me2}** in THF solution together with $\text{VO}(\text{OCH}_3)_3$ overnight leads to a dark red solution from which red crystals could be obtained after work up. An X-ray diffraction analysis of a selected single crystal revealed the molecular structure of the first dinuclear calix[4]arene complex, $[\mu\text{-O}(\text{O}=\text{V}(\text{OMe}))_2\text{B}^{\text{Me2}}]$, **4^t** (see Scheme 6 and Figure 4).

The vanadium centers each form only one bond to **B^{Me2}**. They are coordinated by one aryloxy group with an (ar) $\text{C}-\text{O}-\text{V}$ angle that is characteristic of the paco conformation; nonetheless, the paco conformation is not adopted here, because none of the vanadium centers has a central position. They have moved toward the lower rim being bridged by an oxo ligand. The residual coordination sphere is completed for each V center by one methoxy and one terminal oxo ligand, so that the geometries around the V atoms can be assigned as being tetrahedral. There is no bonding interaction between the V atoms and the methoxy groups of the ligand **B^{Me2}**, as indicated by their distances to vanadium, which are longer than the van der Waals distances. A crystallographic C_2 axis runs through the bridging O5 atom

(24) Liu, L.; Zakharov, L. N.; Golen, J. A.; Rheingold, A. L.; Watson, W. H.; Hanna, T. A. *Inorg. Chem.* **2006**, *45*, 4247.

Scheme 6



and the center of the “calyx”. The distance between the two vanadium centers amounts to 3.3060(2) Å. NMR spectroscopic studies with the bulk product showed that the reaction in Scheme 6 leads not only to 4^t with the two V-bound methoxy groups in trans orientation as in Figure 4 but also to an isomer 4^c where they show a cis positioning (product ratio 3:2). This clearly becomes evident from 1H NMR spectra recorded in C_6D_6 and $CDCl_3$. As mentioned already 4^t displays a C_2 axis, whereas 4^c exhibits a mirror plane through the two methoxy units and the bridging O atom. This leads for both isomers to two different types of methylene groups and thus, as observed and resolved in $CDCl_3$ solution, to two pairs of doublets that can be easily assigned to the individual isomers according to their intensity. For 4^t , two different types of *t*Bu signals are expected, whereas 4^c should show three signals with an intensity ratio of 2:1:1. These signal sets can be found in the experimental spectrum, too, displaying the expected ratios. Furthermore, in the region of the aryl-bound methoxy groups, three singlets can be observed, two of them showing equal intensity. Indeed, in 4^c , these methoxy groups should be magnetically different so that two signals are expected, whereas they are equivalent in 4^t , leading to only one singlet. The vanadium bound methoxy groups are equal in both 4^t and 4^c , leading to two singlets in a 3:2 ratio. The region of the aryl protons cannot be resolved in $CDCl_3$ because of overlap, but the

individual signals appear separated from each other in C_6D_6 . Three signals are apparent with an intensity allowing an assignment to 4^c : two doublets and a broad singlet with doubled intensity. This can be explained as follows: the two vanadium-ligated phenolic moieties are equivalent, so that both show the same sets of signals. However, the protons within each of those phenoxy groups are diastereotopic, showing different chemical shifts; they couple with each other to give two doublets. The aryl protons within the two remaining aryl groups are equal, giving rise to singlets; the two aryl rings differ from each other only slightly so that the expected two singlets overlap to give a broad signal with doubled integral. In 4^t , there is no mirror plane running through any of the aryl rings so that within each ring, the two protons present are magnetically inequivalent. In turn, pairwise, two of the aryl groups are equivalent; in total, 4 doublets with equal intensity should be expected, as observed. From one experiment to the other, the relative yield of 4^t to 4^c varies somewhat, as evidenced by NMR spectroscopy. Samples showing different ratios do not adjust within a couple of hours, which already indicates that the isomers are not in a rapidly adjusting equilibrium to each other. Heating to 60 °C did not alter their ratio. The ^{51}V NMR signals for 4^t and 4^c are coincidentally isochronic (which is not surprising, as the surroundings of the vanadium centers vary only slightly in the second coordination sphere), so only one signal is observed. The chemical shift of -542 ppm compares best with that of **2**, whose vanadium center also shows a tetrahedral coordination sphere. In conclusion of these investigations, it can thus be stated that 4^t also retains the structure it shows in the solid state; on this basis, it can be safely assumed that the same is true for 4^c .

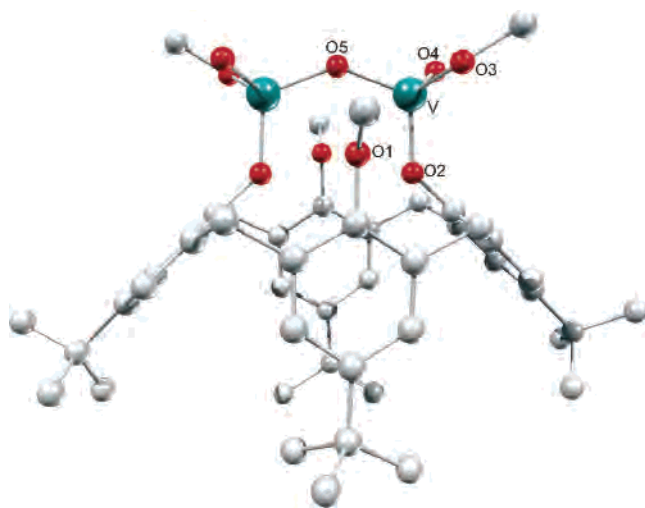


Figure 4. Molecular structure of complex 4^t . All hydrogen atoms were omitted for clarity. Selected bond distances (Å) and angles (deg): O1–V, 3.056(2); O2–V, 1.788(4); O3–V, 1.756(4); O4–V, 1.593(4); O5–V, 1.766(2); O2–V–O3, 110.3(2); O2–V–O4, 108.4(2); O2–V–O5, 113.44(7); O3–V–O4, 104.3(2); O3–V–O5, 111.79(13); O4–V–O5, 108.1(1); V–O5–V', 138.796(3); O3–CH₃, 1.455(8); V–O3–CH₃, 130.1(4); VO2–V'O2', 9.86(9); Ar(O1)–Ar(O1'), 9.5(2); Ar(O2)–Ar(O2'), 88.0(2).

Reactivity of Compounds 1–4 with Respect to the Activation of O_2 for the Oxidation of Alcohols. As outlined in the Introduction, the most prominent conversions that can be carried out using vanadia on oxidic supports as heterogeneous catalysts are the ODH of methanol and alkanes.^{4,5,25} Naturally, molecular models such as those described here will prove themselves unreactive in contact with alkanes, as the rate determining step of the ODH is the first C–H bond cleavage being characterized by a large activation barrier (heterogeneous catalysis at elevated temperatures is required). However, methanol and higher alcohols are less inert as substrates, so their reactions can also be investigated with molecular compounds in the liquid phase. Any information derived from such studies might contribute to a more

(25) Döbler, J.; Pritzsche, M.; Sauer, J. *J. Am. Chem. Soc.* **2005**, *127*, 10861.

Table 2. Substrate Oxidation with O₂ and 1 mol % **1–4** as Catalysts

	TOF (h ⁻¹)					yield (%) after 3 h ^a				
	PPh ₄ ⁺	2	3	4	VO(acac) ₂	PPh ₄ ⁺	2	3	4	VO(acac) ₂
cyclohexanol	0	0	0	0	0	0	0	0	0	0
1-hexanol	0	0	0	0	0	0	0	0	0	0
2-pentanol	0	0	0	0	0	0	0	0	0	0
benzyl alcohol	0	0	3.3	0	12.3	0	0	10	0	13
cinnamyl alcohol	0	1.7	7.0	20.3	50.0	0	5	21	61	100 ^b
crotyl alcohol	0	0	0	0	9.0	0	0	0	0	27
1-phenyl-1-propargylic alcohol	0.7	2.3	25.7	15.3	60.0	2	7	77	46	100 ^c
1-phenyl-1-propanol	0.3	0.7	0.7	1.3	2.7	1	2	2	4	8
9-fluorenone	0	3.0	86.0	15.3	24.0	0	15	100 ^d	46	72
9,10- <i>H</i> -dihydroanthracene	0	0.7	10.0	1.3	0	0	2	30	4	0
fluorene	0	0	0	0	0	0	0	0	0	0

^a The numbers in the right column specify the yield of oxidation product referring to the alcohol. ^b 50% yield after 1 h. ^c 60% yield after 1 h. ^d 86% yield after 1 h.

comprehensive understanding of the methanol oxidation at vanadia catalysts and they might as well provide ideas concerning the (probably) more complex ODH of alkanes.

To test the compounds described above for any reactivity in relation to the ODH and to thus test them as models, we therefore decided to investigate the oxidation of a palette of various different alcohols with O₂ as the reagent. Of course, there are numerous methods to oxidize alcohols with organic or inorganic reagents,²⁶ which, however, are often stoichiometric and/or lead to toxic waste products. The performance of catalytic oxidations with O₂ is therefore still an attractive topic, and a lot of research has been devoted to it in the past.²⁶ Certainly, the background of the study presented here, as mentioned, was an inquiry into whether compounds **1–4** could represent not only structural but also functional models for the heterogeneously catalyzed ODH and not the improvement of known catalysts for the aerobic oxidation of alcohols. Nevertheless, the latter aspect was borne in mind as a potential, beneficial quality of the investigation.

As we are dealing with V^V compounds that are discussed as functional models, they should contain functional moieties already, i.e., the first step of a possible catalytic cycle should consist of a reaction with the chosen alcohol. After a potential oxidation reaction, O₂ could serve to regenerate the active species (for an initial O₂ activation, some d-electrons would be required: d⁰ complexes mostly do not activate O₂). As a reference, a system was chosen that has been shown to catalyze the aerobic oxidation of 1-phenyl-1-propargylic alcohol:²⁷ OV(acac)₂, which probably belongs to the category of complexes that activates O₂ first.

Catalytic amounts of the synthesized complexes were dissolved in acetonitrile, and molecular sieve was added to remove the water being produced during the oxidation. After the addition of a chosen alcohol, the resulting mixture was heated for 1–3 h at 80 °C under an oxygen atmosphere. After work up, the turnover frequencies (TOFs) were determined by NMR spectroscopy. The results are summarized in Table 2. Three aliphatic alcohols were employed: 1-hexanol, 2-pentanol, and cyclohexanol. No con-

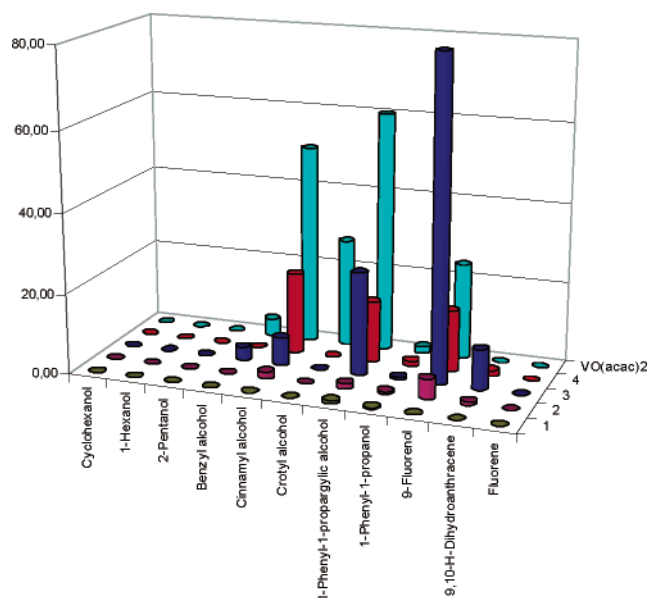


Figure 5. Substrate oxidation with O₂ catalyzed by complexes **1–4**. The numbers refer to TOFs (h⁻¹).

version could be observed for any of them, neither with complexes **1–4** nor with the reference system. In case of 1-hexanol, this was not too surprising, as it represents a primary alcohol, the oxidation of which is difficult with vanadium compounds. Nonetheless, for **3**, we were able to observe some activity in the oxidation of other primary alcohols, namely, in the cases of benzyl alcohol and cinnamyl alcohol (TOFs of 3.3 and 7.0 h⁻¹, respectively), and OV(acac)₂ performed even better (12.3 and 50.0 h⁻¹), being capable of oxidizing crotyl alcohol in addition with a TOF of 9.0 h⁻¹. When 1-phenyl-1-propargylic alcohol and fluorenone were employed, the following picture emerged: mononuclear complexes **1** and **2** led to only low conversions. However, the dinuclear complexes and the reference system led to much higher TOFs between 15 and 86 h⁻¹. With a TOF of 86 h⁻¹, the activity of **3** for the oxidation of fluorenone was even almost 4 times higher than the one of OV(acac)₂.

These findings could hint to the fact that two vanadium centers are advantageous for an efficient catalysis and that the activity of OV(acac)₂ has the formation of a dinuclear active species in solution as its basis.

- (26) Arends, I. W. C. E.; Sheldon, R. A. In *Modern Oxidation Methods*; Bäckvall, J.-E., Ed.; Wiley-VCH: Weinheim, Germany, 2004; p 83.
 (27) Maeda, Y.; Kakiuchi, N.; Matsumura, S.; Nishimura, T.; Kawamura, T.; Uemura, S. *J. Org. Chem.* **2002**, *67*, 6718.

Having found that some of the complexes do in fact show activity as catalysts for the alcohol oxidation, a nonfunctionalized hydrocarbon was then employed to further exploit their potential. A substrate with comparatively weak C–H bonds was chosen, namely, 9,10-dihydroanthracene. Remarkably, the two dinuclear complexes **3** and **4** again proved to be active (even though the TOFs were much lower in comparison to those for the alcohols), whereas the reference system proved to be inactive. The oxidation products were identified as 10% (3%) anthracene, 13% (6%) 10*H*-anthracene-9-one, and 7% (6%) 9,10-dihydroanthracene-9,10-diol. These oxidations probably proceed via anthranol and dihydroanthracenediol by analogy with a corresponding oxidation using a Ru catalyst.²⁸ However, when fluorene, whose C–H bonds are somewhat (ca. 23 kJ/mol) stronger, was chosen as the substrate, none of the compounds employed showed any activity.

The mechanism of oxidation for the catalysts employed is still unclear (possibly, there is more than one). As mentioned above, the first step in the cases of the active V^V catalysts will consist of a reaction with the alcohol, and in fact, a significant color change can be observed on addition of the alcohol for the active catalysts. A further color change can then be noted on heating, together with O₂. However, so far, we have not been able to identify any of the potential intermediates. More detailed and extensive studies might provide some insight in future. Nevertheless, the results of these preliminary investigations put forward some interesting working hypotheses concerning the prerequisites for successful catalysis (e.g., with respect to nuclearity) that will be tested in subsequent research.

Somewhat irritating was the apparent inertness of complex **1** that, at first sight, had not been expected. Therefore, some further reactivity studies were performed. First of all, stoichiometric reactions with tetramethylethylene, dihydroanthracene, and alcohols were performed. **1** was then tested as catalysts for the oxidation of these hydrocarbons with O₂ in the presence of reducing agents such as Zn or Mg, and finally as catalyst for the photooxidation of benzene and cyclohexene with O₂. In all these experiments, **1** behaved inert, and

it turned out that it does not even transfer the terminal oxo ligand to phosphines. A possible reason lies in the negative charge that has to be accommodated for an O=V³⁺ unit if it is surrounded by four additional negatively charged ligands, and this conclusion could also hold for corresponding surface species.

Conclusions

The synthesis and characterization of two mononuclear and two dinuclear oxo vanadium calixarene complexes (charged as well as neutral) have been achieved. Some of these complexes proved to be efficient catalysts for the O₂ oxidation of activated alcohols. It could be noted that the two dinuclear complexes were significantly more active than the two mononuclear compounds. Subsequent studies even showed that the singly charged mononuclear complex **1** behaves completely inert toward other substrates under various conditions, whereas the two dinuclear complexes were capable of oxidizing a nonfunctionalized hydrocarbon like 9,10-dihydroanthracene, although the TOFs are much lower in comparison to the ones for the alcohol oxidations. These findings may have implications on the discussion which kind of species are active in oxidative dehydrogenations with vanadia catalysts, as they suggest an increase in activity through the cooperative behavior of two metal centers. However, a larger number of complexes has to be synthesized and more detailed mechanistic investigations have to be performed to support this hypotheses. Especially, the identification of an oxidation intermediate would be very helpful. Current work deals with these issues.

Acknowledgment. We are grateful to the Deutsche Forschungsgemeinschaft, the SFB 546, the Fonds der Chemischen Industrie, the BMBF and the Dr. Otto Röhm Gedächtnisstiftung for financial support. We also thank C. Jankowski for the preparation of starting materials and C. M. Klemm for performing catalytical tests.

Supporting Information Available: X-ray crystallographic data in cif format and plots of the crystal structures showing the 30% probability level ellipsoids. This material is available free of charge via the Internet at <http://pubs.acs.org>.

IC061106J

(28) Kamata, K.; Kasai, J.; Yamaguchi, K.; Mizuno, N. *Org. Lett.* **2004**, *6*, 3577.